Available online at www.sciencedirect.com

ScienceDirect

Procedia Engineering 166 (2016) 190 – 201

Procedia Engineering

www.elsevier.com/locate/procedia

2nd International Symposium on Submerged Floating Tunnels and Underwater Tunnel Structures

On mode competition during VIVs of flexible SFT's flexible cylindrical body experiencing lineally sheared current

Weimin Chen[a]*,Yilun Li[b], Yiqin Fu[a],Shuangxi Guo[a]

[a]*Key Laboratory of Mechanics in Fluid Solid Coupling System, Institute of Mechanics, Chinese Academy of Sciences, Beijing 100190, China*
[b]*Sino-French Engineering School, Beijing University of Aeronautics and Astronautics, Beijing 100191, China*

Abstract

Most of the floating tunnel and supporting tendon or cable of submerged floating tunnel (SFT) are essentially cylindrical body. Multi-mode vortex-induced vibration (VIV) of these flexible bodies frequently happens in non-uniform flow due to structural flexibility and non-uniform distribution of fluid velocity. One of the challenging issues of multi-mode VIV is about mode competition. And the mechanism and its quantitively measurement of mode competition, in terms of excitation region and length of potentially participating modes along with modal weights, become more complicated than single-mode VIV.

In this study, mode competition and multi-mode VIV of flexible body in lineally sheared current is explored based on our numerical simulations which combine finite element approach with a hydrodynamic model so as to carry out nonlinearly simultaneously dynamic response in time domain. Our numerical results show that multi-mode VIV may occur both in non-uniform and uniform fluid profiles. In sheared current, as the towing speed (or the maximum speed) increases, because more modes with higher modal order number participate into the dynamic response, the average RMS displacement just change a little while the average RMS stress progressively rises. Moreover, there are different dominant frequencies distributing along cylinder span, and the length of the first dominant frequency gets smaller due to larger shearing parameter along with more intense competition between all participating modes.

Peer-review under responsibility of the organizing committee of SUFTUS-2016

Keywords: submerged floating tunnel (SFT); flexible cylindrical body; vortex-induced vibration (VIV); multi-mode

* Corresponding author. Tel: 86-10-82543891, Fax: 86-10-82338967.
E-mail address: wmchen@imech.ac.cn.

Peer-review under responsibility of the organizing committee of SUFTUS-2016
doi:10.1016/j.proeng.2016.11.582

1. Introduction

Most of the floating tunnel and supporting tendon or cable of submerged floating tunnel (SFT) are likely to be cylindrical body which is essentially slender and flexible. Moreover, the shedding mode or frequency of wake vortex may vary, or even be grouped in cells, along cylinder span due to span-wise coupling of vortices[1-2]. Therefore, multi-mode vortex-induced vibration (VIV) of these flexible bodies frequently occurs in non-uniform current due to structural flexibility and non-uniform distribution of fluid velocity. One of the challenging issues of multi-mode VIV is about mode competition. And, the mechanism and its quantitively measurement of mode competition, in terms of excitation region and length of potentially participating modes along with modal weights, become more complicated than single-mode VIV.

In recent years, increasing researches about multi-mode VIV have been reported[3-13]. Based on large-scale tests performed at Hanotangen outside Bergen of Norway [4], Lie and Kaasen[5] studied if and under which circumstances the VIV would be single-mode or multi-mode. They found that, for case of well-defined shear flow, in general the response was irregular (i.e. broad-banded) and that the degree of irregularity increases with the flow speed. No occurrences of single-mode (lock-in) were seen. In some tests distinct spectral peaks could be seen, corresponding to a certain dominant mode. Huera-Huarte et al.[8] provided the force distribution based on measured displacement of a vertical tension cylinder in a stepped current by employing an indirect technique that uses experimental data and finite element method. His experimental data demonstrated a correlation between the mean drag and the transverse response along a cylinder undergoing multi-mode vibration. Huang et al.[9] used measurement data of long flexible cable models undergoing multi-mode VIV in uniform current to study the drag amplification taking into account of the spatial variation of vibration amplitude along cable span.

Still, there are some problems remain interesting. For examples, multi-mode VIV was mostly found in non-uniform fluid profile, does it also occur in uniform flow? Further, in shear flow, as the shearing intensity changes, what will happen to the VIV of slender cylinder, in terms of displacement, stress and/or participating mode? In this study, multi-mode VIV of flexible cylinder in different shear fluid profiles, i.e. shear flows with different shearing intensities, is examined based on our numerical simulations which combine a hydrodynamic model with finite element method to carry out nonlinearly simultaneously dynamic response in time domain. The effects of towing speed on displacement, stress and participating mode (or frequency) distribution along cylinder's span are studied.

2. Numerical simulation based on hydrodynamic model and FEM

The governing equation of a cylindrical body, generally regarded as a tensioned Euler beam, undergoing VIV can be written as

$$m\frac{\partial^2 y(z,t)}{\partial t^2}+\gamma\frac{\partial y(z,t)}{\partial t}+EI\frac{\partial^4 y(z,t)}{\partial z^4}-T\frac{\partial^2 y(z,t)}{\partial z^2}=f(z,t) \qquad (1)$$

where $y(z,t)$ is the structural displacement, m and γ are the structural mass and damping per unit length; EI and T are the bending stiffness and axial tension. $f(z,t)$ is the hydrodynamic force per unit length consisting of the vortex-induced lift force $f_L(z,t)$ and fluid drag force $f_F(z,t)$. For a body undergoing both the drag force and vortex-induced lift force, to get the theoretical solution of its dynamic response is pretty difficult. Thus a numerical approach based on finite element method and the hydrodynamic model is employed here.

2.1. Structure model based on FEM

The cylinder is uniformly divided into N elements which are two-node Euler beam element. For representativeness and simplicity, only one translation displacement y_i, $i=1,2,\ldots,N+1$ (N+1 is the total number of

nodes), and one rotation θ_i, $i=1,2,\ldots,N+1$, of per node, are considered. The displacement function of the beam element is written as

$$y(\xi)=\sum_{i=1}^{2}\varphi_i^0(\xi)y_i+\sum_{i=1}^{2}\phi_i^1(\xi)\theta_i \tag{2}$$

$$\varphi_1^0(\xi)=1-3\xi^2+2\xi^3 \quad \varphi_2^0(\xi)=3\xi^2-2\xi^3$$

$$\varphi_1^1(\xi)=(\xi-2\xi^2+\xi^3)/l_e \quad \varphi_2^1(\xi)=(\xi^3-\xi^2)/l_e$$

where ξ is the internal coordinate of beam element, $\xi=(z-z_1)/L, \quad 0\le\xi\le 1$. l_e and L are the element length and overall cylinder's length respectively. The element mass matrix $\mathbf{M}^e$, stiffness matrix $\mathbf{K}^e$ and geometry stiffness matrix $\mathbf{K}_t^e$ are respectively:

$$\mathbf{M}^e=\int_{l_e}\rho\boldsymbol{\varphi}^T\boldsymbol{\varphi}d\xi \quad \mathbf{K}^e=\int_{l_e}\mathbf{B}^T D\mathbf{B}d\xi \quad \mathbf{K}_t^e=\int_{l_e}\bar{\mathbf{B}}^T\bar{\mathbf{B}}d\xi$$

where $\boldsymbol{\varphi}=\begin{bmatrix}\varphi_1^0 & \varphi_1^1 & \varphi_2^0 & \varphi_2^1\end{bmatrix}$ is the element deformation function. Coefficient matrices $\mathbf{B}=d^2\boldsymbol{\varphi}/dx^2$, $\bar{\mathbf{B}}=d\boldsymbol{\varphi}/dx$ and $D=EI$.

Then the governing equation of the cylinder with multi-degree of freedom can be written as follow:

$$\mathbf{M}\ddot{\mathbf{Y}}+\mathbf{C}\dot{\mathbf{Y}}+\mathbf{K}\mathbf{Y}=\mathbf{F} \tag{3}$$

M, **C** and **K** are the structural mass, damping and stiffness matrix respectively, which are assembled by the corresponding element matrices. **Y** and **F** are the displacement and load vector of the nodes.

For case of small structural damping, the Rayleigh damping can be used and is written as a linear combination of mass matrix **M** and stiffness matrix **K** as follows

$$\mathbf{C}=a\mathbf{M}+b\mathbf{K} \tag{4}$$

where a and b are positive constants of which values can be determined by experiments, or approximately, the natural frequencies of structure as follows:

$$a=\frac{2\omega_1\omega_2(\zeta_1\omega_2-\zeta_2\omega_1)}{\omega_2^2-\omega_1^2}, \quad b=\frac{2(\zeta_2\omega_2-\zeta_1\omega_1)}{\omega_2^2-\omega_1^2} \tag{5}$$

Where ζ_j, and ω_j $(j=1,2)$ are respectively damping ratio and natural frequency of mode j. Generally, the value of structural modal damping ratio is 3 percent, or $\zeta_1=\zeta_2=0.03$.

The vortex-induced lift force $f_v(z,t)$ and the drag force $f_f(z,t)$ exerted by the ambient fluid are applied at the nodes respectively in the excitation and damping region along the cylinder length. The element load in terms of element node is $\mathbf{F}^e=\int_{l_e}q\boldsymbol{\varphi}^T d\xi$. Element mass are equally divided at two nodes of each beam element.

2.2. Hydrodynamic model considering the interaction between structural and fluid dynamics

The fluid drag force $f_F(z,t)$ can be expressed by virtue of the Morison equation, i.e.

$$f_F(z,t)=\frac{1}{2}C_D\rho_f D\dot{y}(z,t)\left|\dot{y}(z,t)\right|+\frac{1}{4}\pi C_A\rho_f D^2\ddot{y}(z,t) \tag{6}$$

where ρ_f and V are the density and velocity of fluid respectively, and D is the diameter of the cylinder. C_D and C_A are the drag and added mass coefficients respectively, of which the values are $C_A=1.0$ and $C_D=1.1$ for a flexible cylinder with large aspect ratio.

The expression of vortex-induced lift force f_L is more complicated because VIV has always been a challenging issue concerning the interaction between fluid and structural dynamics. Initially, vortex-induced lift force per unit length of structure is written, somewhat similarly with the Morison's equation, as $f_L=(1/2)\rho_f U^2 C_L D$ where the lift coefficient C_L is a constant value ranging from 0.5 to 1.2. Recently, with increasing amount of experimental observations in laboratories or large-scale fields[4,5,14] along with CFD simulations, new approaches of lift force during lock-in were proposed, which are more accurate and reasonable because coupling between structural and fluid dynamics were taken into accounts[3,15,16]. Sarpkaya[15] experimentally measured the Fourier average of hydrodynamic force over many cycles of vibration. He decomposed the lift force into two parts, the drag part and the inertia part, which are respectively related to the velocity and acceleration of the vibrating cylinder. He pointed out that for practical Reynolds numbers, the nonlinear expression with respect to structural motion is able to capture the hydrodynamic feature better than the linear expression. Vandiver and Li[16] suggested that a piecewise parabola function of structural amplitude could be used for industrial model of lift force to calculate structural displacement by using modal superposition model.

Here, the third-order polynomial of the structure velocity originally suggested by Chen[3] is used to model the lift coefficient so as to take account of nonlinear interaction between structural and fluid dynamics, i.e.

$$f_L(z,t)=p_f C_{L0}\sin(\omega t)+p_f C_1\dot{y}(z,t)+p_f C_2\dot{y}^2(z,t)+p_f C_3\dot{y}^3(z,t)) \tag{7}$$

where $p_f=(1/2)\rho_f D V^2$. The values of coefficients C_{L0}, C_1, C_2 and C_3 can be derived by fitting experimental data. Chen[20] gave an approach to calculate the coefficients' values by fitting experimental data. Observing Eq. (7), we may say it is able to capture, to some extents, features of VIV. For examples, the feature of self-excitation is represented by the first term $p_f C_{L0}\sin(\omega t)$, a sinusoidal excitation force, together with the second term, $p_f C_1\dot{y}(z,t)$, which increases as response increases (C_1 is required to be positive); the feature of self-limitation, i.e. structural response never rises infinitely, but begins to drop when its value reaches to a certain number ($\overline{y}_{\max}=1.5$ or 2.0) is represented by the nonlinear terms with higher orders of structural motion in Eq.(7), $\rho_f C_2\dot{y}^2(z,t)$ or $\rho_f C_3\dot{y}^3(z,t)$ (at least one of the coefficients C_2 and C_3 is negative). And, this model, in some way, automatically captures the span coherence behavior of a flexible cylinder's VIV because the lift force is non-uniform owing to the axially varying amplitude of cylinder's response.

2.3. Mode competition and dynamic response of the coupling system

When it comes to the mechanism of multi-mode participation or mode competition, it is still somewhat unclear. Jaiswal and Vandiver[10] used the concepts of ''time sharing'' to describe the ''mode switching'' along the time coordinate for a shear velocity profile, while Tognarelli et al.[11] called it ''space sharing''. Violette et al.[16] performed a linear stability approach to identify the mode switching of two excited modes in cable VIV. He theoretically explained this behavior based on the linear stability approach, regarding different modes can be excited at different and coincident time instants. Marcollo and Hinwood[12] experimentally examined the area where a

cylinder's VIV can vary from single mode lock-in to multimodal. He found an interesting and unexpected mechanism of multi-mode vibration, that higher frequency mode's damping region may provide a power-in effect to support other mode's response. Zhang et al.[13] studied multi-mode vibration of mooring-line, and his results showed that the unstable zone significantly grows and a small excitation can induce large dynamic response for a multi-mode coupled system. Srinil[7] studied multi-mode interactions of VIV in uniform current by using semi-empirical wake oscillator model. He thought multi-mode lock-in, switching, sharing and interaction features take place both in response time histories (for a given flow velocity) and amplitude diagrams (with increasing flow velocity). In amplitude diagrams, multiple modal responses overlap in specific velocity ranges. The lock-in band width is found to be mode-dependent.

As for the excitation region along cylinder length in which vortex-induced lift force is loaded, for case of single-mode VIV, the modal excitation location can be simply determined as long as the modal reduced velocity $V_{rn}(z,n) = V(z)/Df_n$ at location z along the cylinder length falls into the range of lock-in velocity, i.e. $4 \le V_{rn}(z) \le 12$. However, for case of multi-mode vibration, at location z, there may exist multiple participating modes of which the modal reduced velocities all satisfy $4 \le V_{rn}(z) \le 12$. In other words, overlap between adjacent excitation regions may occur if several modes simultaneously participate in the vibration. What's more, for case of shear flow, the overlap is more complicated due to the non-uniform distribution of the reduced velocity along cylinder length.

To eliminate the overlap, we use the modal competition to measure excitation region so that the mode being more powerful would be more likely to participate into the vibration, or even, finally would become the dominant mode. Analyzing the modal data of VIV tests[5, 21], we would assume that there are competitions between all potentially participating modes. In other words, the mode that holds more power would be more likely to participate into the vibration and, even, finally to become the dominant mode. For example, VIV experiments implied that with the change of reduced velocity from 4 to 12 the participating modes varied from mode 20 to 10. Moreover, appearance of a new excitation mode is usually accompanied by disappearance of previously existing modes. Or, the new excitation mode with increasingly large power could overcome the previous one with decreasing power until it disappears in overall dynamic response (see the Figs. 9, 15 and 16 there in the paper by Chaplin et al.[21].

And, based on the large-scale tests in shear flow[4,5], we noted that the modal weights of all participating modes distribute unequally and, often, there are a few modes (e.g. around 1~3 modes) mainly dominating the vibration response (or with higher values of modal weight). Thereby, we may say that the weight of one participating mode should be related to the modal energy of this mode [Chen et al., 2016], which is written as:

$$P_n = [\int_{L_n} \frac{1}{2} C_L \rho D V^2(z) \varphi_n^2(z) dz]^2 \Big/ \int_{L-L_n} r_h(z) \varphi_n^2(z) dz + \int_L r_s(z) \varphi_n^2(z) dz \qquad (8)$$

where $r_h(z)$ and $r_s(z)$ are the hydrodynamic and structural damping respectively. L_n is the modal excitation length according to the reduced velocity. $\phi_n(z)$ is the modal shape. Since the location of excitation force is one of important factors that influence modal excitation energy, i.e. the excitation force applied at anti-node of this mode would give a much larger response displacement than the force at the node. Thus, modal shape $\phi_n(z)$, representing the location of force, is involved in the integration of Eq. (8). It is assumed that the original length of excitation region for participating modes should shrink, in a way of inversely proportional to its modal energy, till the overlap disappears, i.e. $L_n/L_{n+1} = P_n/P_{n+1}$.

Additionally, the rule to select the modes that are most likely to participate into the dynamic response is assumed as follows: the first six modes which have the largest values of modal energy are selected as participating modes; or, if the modal energy is 85 percent lower than the first mode, those modes will be neglected.

Finally, based on the structural and hydrodynamic models presented above, a nonlinear simultaneously dynamic response can be analyzed. Regarding the nonlinear load and central mass in terms of element nodes, direct numerical integration is used to solve the dynamic governing equation, Eq.(3). The fundamental structural displacement is solved at discrete times with a fixed integration times step Δt ($\Delta t \le T_{\min}/50$, $T_{\min}$ is the minimum natural period of all participating modes). By using a Newmark-Beta representation for the velocity and the displacement at discrete times

$$\{\dot{y}_{t+\Delta t}\} = \{\dot{y}_t\} + [(1-\delta)\{\ddot{y}_t\} + \delta\{\ddot{y}_{t+\Delta t}\}]\cdot\Delta t$$

$$\{y_{t+\Delta t}\} = \{y_t\} + \{\dot{y}_t\}\cdot\Delta t + [(\tfrac{1}{2}-\alpha)\{\ddot{y}_t\} + \alpha\{\ddot{y}_{t+\Delta t}\}]\cdot\Delta t^2$$

, the dynamic equation can be solved by Newmark-Beta direct integration method so as to effectively and economically run the dynamic analysis.

The initial condition is that both the initial displacement and velocity are zero. The boundary conditions at the two pinned ends of the cylinder are:

$$\begin{aligned} &x(0,t) = 0 \qquad && x(L,t) = 0 \\ &\partial^2 x(0,t)/\partial z^2 = 0 \quad && \partial^2 x(L,t)/\partial z^2 = 0 \end{aligned} \tag{9}$$

3. Multi-mode VIV responses and its discussions

3.1. Verification and comparison of multi-mode and single-mode VIV in uniform and non-uniform currents respectively

Our numerical results of both multi-mode and single-mode VIV are compared with the experimental results, i.e. a flexible cylinder in uniform flow by Trim et al.[22] and a flexible cable in non-uniform flow by Huse et al.[4].

For the flexible cylinder in uniform flow (see Fig.1), two dynamic responses, i.e. the single-mode vibration involving only the mode 3 and the multi-mode vibration involving the modes 3 and 4, are carried out. The numerical results, plotted as the RMS of displacement along cylinder length and the temporal-spatial evolution of displacement, are shown in Fig. 1a and 1b respectively. Generally speaking, the displacement of multi-mode agrees with the experiment better than the single-mode.

In Fig.1a, the dominant mode of either multi-mode or single-mode response are consistent with the experimental mode (mode 3). However, if comparing the RMS displacement, there are differences between the two dynamic responses. For example, the span-averaged RMS displacements (scaled by the diameter of the cylinder as the non-dimensional *y/D*) are respectively 0.36 (multi-mode) and 0.34 (single-mode) compared with 0.39 of the experiment. The averaged-value of the 3 peaks are respectively 0.48 (multi-mode) and 0.54 (single-mode) compared with 0.50 of the experiment. The average values of the two troughs of single-mode is just 0.0068 that is much lower than the experimental value 0.32 while the multi-mode value is 0.26. That is to say for single-mode VIV the RMS displacement near the peaks is approximately close to the experiments, whereas the displacements at other positions, especially near the two troughs, distinctly diverge from the experiments. If comparing the phase, there is no significant difference between the two cases, e.g. the offset of peak (or trough) location from the experiment for the two cases are around 7-10%.

Observing the temporal-spatial evolutions of the displacement, in Fig.1b, slight travelling wave is seen in multi-mode VIV, similarly, no evident node can be seen there in the solid line in Fig.1a, and that is consistent with the experiment.

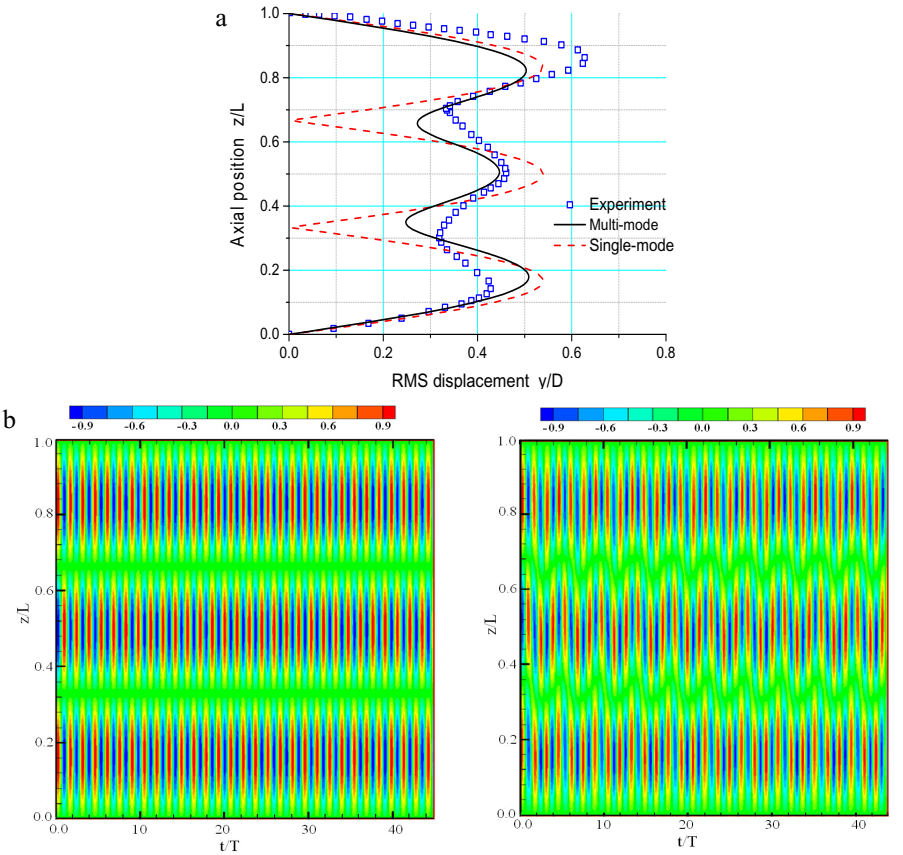

Fig.1 Multi-mode and single-mode VIV of a flexible cylinder in uniform fluid profile, based on our numerical simulations against the experimental results (a) The RMS displacements (b) The temporal-spatial evolution of displacement

For case of flexible cylinder in non-uniform flow, we chose the large-scale field experiments [10] of which the aspect ratio is quite large (3000) as our example model to explore its multi-mode VIV. The VIV responses at ten towing speeds were simulated by our FEM simulations. Here selected results, at two typical towing speeds of 0.54m/s and 1.14m/s, are presented.

The RMS displacement along the cylinder's length is plotted against the experiments in respectively Fig. 2a (at towing speed 0.54m/s) and Fig. 2c (at towing speed 1.14m/s), as a comparison, the single-mode VIV of the dominant mode is plotted as dot lines there too.

Similarly with the case of uniform flow, it is seen that the response, in term of displacement and dominant mode, of the multi-mode VIV agree with the experiments much better than the single-mode VIV. Taking the speed of 0.54m/s as an example, the span-averaged RMS displacements are respectively 0.0073m (multi-mode) and 0.0065m (single-mode) compared to 0.0075m of the experiment. The averaged values of the peak-displacements are respectively 0.0090m (multi-mode) and 0.0091m (single-mode) compared to 0.0088m of the experiment. We note that the trough-averaged values 0.0055m (multi-mode) and 0.0033m (single-mode) somewhat divert from the experiment value 0.0068m by 19.1% and 51.4% respectively. The reason why such apparent difference might be there were more and random modes participated into the response during experiments but selected modes are involved in our numerical simulation.

Considering then the dominating mode and phase, the dominating mode of multi-mode VIV is consistent with the experiment, for example, at towing speed 0.54m/s, the dominating modes of the presented model and experiment are

mode 11 while the dominant mode of single-mode VIV, mode 13, is a little different from the experiment. If comparing the phase, the offset of peak (or trough) location of multi-mode from the experiment are around 7.01 % (or 11.40%) respectively.

Considering last the wave type. Observing the evolution of displacement versus time and cylinder span, or the temporal-spatial displacement plot, see Fig.2b and 2d, the response is a mix of standing wave and travelling wave. Standing wave dominates the two regions which are closer to top or bottom ends. Because in these two regions, it is easier for the excited wave to meet the reflected wave propagating from the end and then to form a standing wave before it declines to small value or zero.

Travelling wave becomes more obvious at higher towing speed (1.14m.s). As we know, the damping effect is faster for the modes with higher modal order than lower order. Thus the modal dynamic response of those higher-order modes declines faster. Or, the vibration excited by higher frequency near top-end may decline rapidly into a pretty little, even zero, value before it reaches the cylinder's bottom end, and then, to reflect backward. Owing to pretty small, or even zero, reflected wave to meet with the approaching wave, the vibration wave would be characterized as travelling wave.

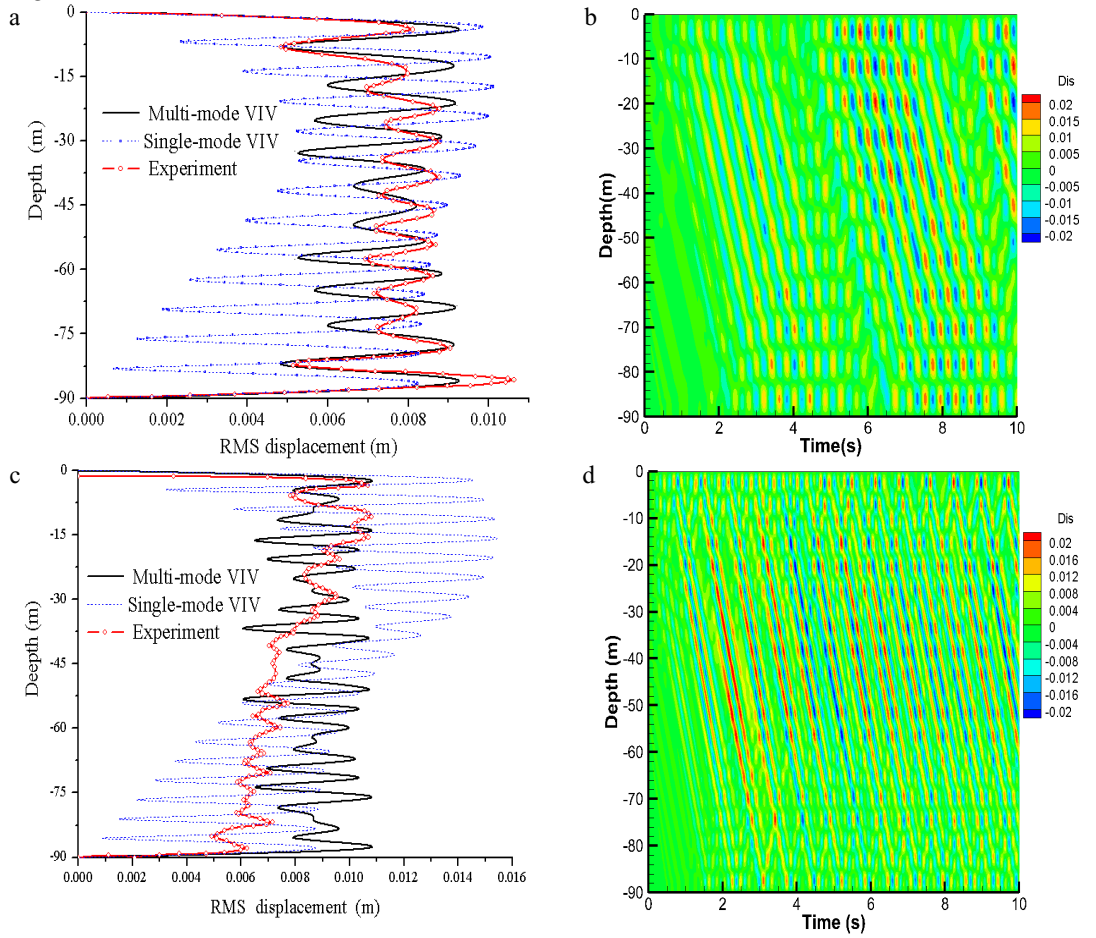

Fig.2 Multi-mode and single-mode VIV of a flexible cylinder in non-uniform fluid profile respectively at the towing speed 0.54m/s and 1.14m/s (a) RMS displacement at towing speed 0.54m/s (b) The temporal-spatial evolution of displacement of the multi-mode VIV at towing speed 0.54m/s. (c) RMS displacement at towing speed 1.14m/s (d)The temporal-spatial evolution of displacement of multi-mode VIV at towing speed 1.14m/s

3.2. Discussions on multi-mode VIV and frequency distribution at different fluid speeds

The time histories and temporal power spectral density (PSD) of the points with the maximum RMS displacement are plotted in Fig. 3. Both cases exhibit vibrations at multiple frequencies but the structural responses differ in the participating mode: as the towing speed increases from 0.54 to 1.14 m/s, the highest modal order increases from 16 to 24, while the band width of mainly excited frequencies broadens, i.e. from 0.99Hz ~3.29Hz (mode 5 ~mode 16) to 0.50Hz~6.29Hz (mode 2 ~mode 24).

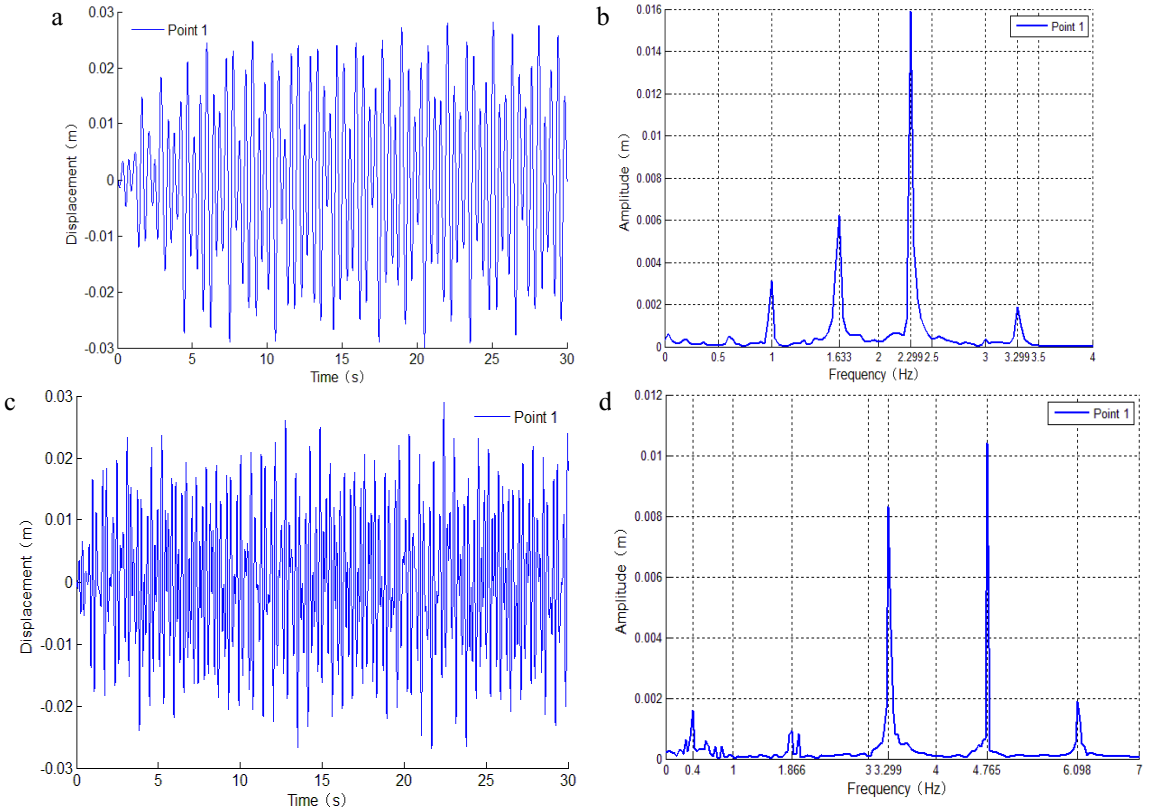

Fig.3 Displacement time history and frequency spectrum of the point with the maximum RMS displacement. (a) Time history at towing speed 0.54m/s. (b) Frequency spectrum at towing speed 0.54m/s. (c) Time history at towing speed 1.14m/s. (d) Frequency spectrum at towing speed 1.14m/s

Interestingly, more and/or higher-order participating modes do not necessarily mean larger displacement, see Fig.4a. The span-averaged RMS displacement is around 0.0078m, e.g. 0.0073m for 0.54m/s towing speed compared with 0.0080m for speed 1.14m/s. As towing speed increases, there are two changes: different modes participate into (or drop out of) dynamic response and the excitation region for a certain mode change too. Thus, these two changes might be responsible for the uncertainty, or slight change rather than gradual rise (or drop), of displacement amplitude.

However, as the towing speed increases, the stress obviously rises, see Fig.4b. New modes with higher-order number are excited while the towing speed increases, of which the modal curvatures, or the modal stress get larger. What's more, the higher level of stress is with higher frequencies owing to higher-order number of participating modes. This will inevitably impact the fatigue performance of structure, which should be a serious concern of SFT's safety assessment.

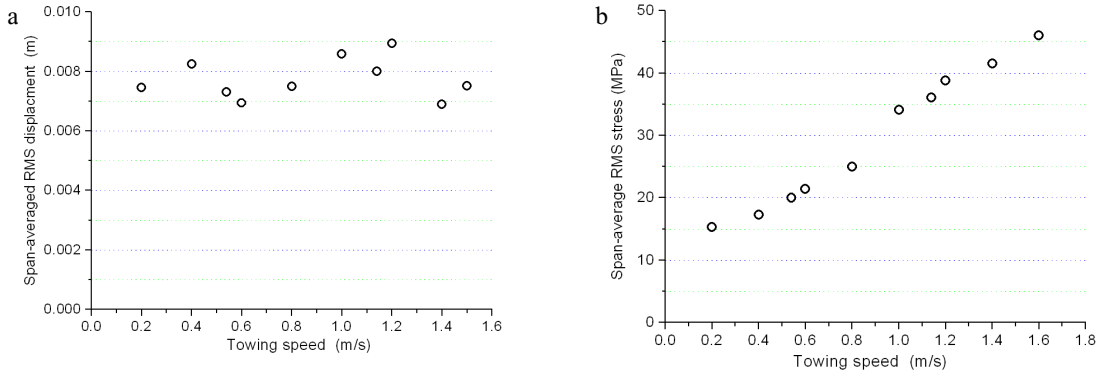

Fig.4 Effects of towing speed on vortex-induced vibration response (a) Average RMS displacement versus towing speed(b) Average RMS stress versus towing speed

The distributions of dominant frequencies along structure length are presented in Fig.5. Several participating frequencies can be identified by distinguishing the frequencies with larger peak value of displacement power spectrum at different points along structure length. Among those peak frequencies, the two frequencies which have the largest two value of dominant length along cylinder span are respectively named the first-dominant and second-dominant frequency, the rest frequencies are named other-dominant frequency.

Comparing the results of the two speeds (Fig.5a and 5b), it is noted that the distributions along cylinder span, in terms of the band width and length of dominant frequencies, varies as the towing speeds rises. Generally speaking, for case of lower speed 0.54m/s, Fig.5a, the first-dominant frequency has the value of 2.30Hz, the frequency of 11th mode, which is also demonstrated in the RMS displacement of Fig. 3a. The first-dominant region ranges from the depth 0.5m to 89.0m. The second-dominant frequency of 1.63Hz, being same with natural frequency of mode 8 of the cylinder, scatters at some points among the first-dominant region, as well other frequencies. This phenomena of multi-frequency dominance along cylinder span was also reported by Lucor et al.[2] and Bourguet et al.[23]. They pointed out that it is because of the shedding cells of vertex which have different shapes and frequencies in the wake filed behind the cylinder undergoing VIV. Here, from our view of structural dynamics, it might because of the multiple modes that simultaneously participate into the response and their nonlinear interactions between each other.

For case of speed 1.14m/s, Fig.5b, the band width of dominant frequencies gets wider and the first and second-dominant frequencies are respectively 4.76 and 3.31Hz which are the natural frequencies of modes 15 and 20. And, what's more, the first-dominant region, 0.5m-78.5m, gets smaller while the second and other dominant frequencies share more region along the cylinder span. It is partly because there are more participating modes, ranging from modes 2-26 compared with modes 3-15 of 0.54m/s speed, into the dynamic response as the towing speed gets larger, in others word, the shear intensity, $(V_{\max} - V_{\min})/L$, get larger. In that case, the modal competition gets fiercer, and it's harder for a dominant mode to occupy most cylinder span or they have to share dominant region somewhat.

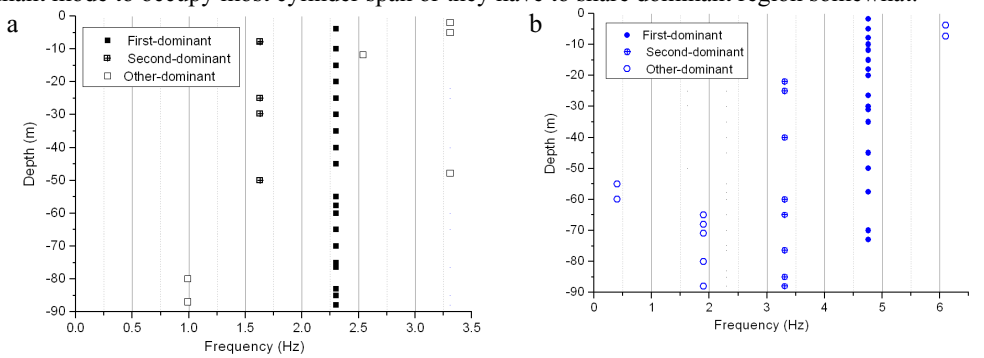

Fig.5 Distributions of dominant frequencies along the cylinder span. (a) At towing speed 0.54m/s; (b) At towing speed 1.14m/s

4. Conclusions

Multi-mode VIV of long flexible cylinder in shear fluid profile is explored, which happens not only in non-uniform flow but also in uniform flow. Our numerical results show that more and higher-order modes take part in the dynamic response as the towing speed increases. And, the average displacement slightly changes while the stress progressively increases, approximately linear, with the increase of towing speed. High-level of stress at higher frequency could be a concern owing to fatigue problem. There are different dominant frequencies distribute along cylinder span, and the length of the first dominant frequency gets smaller due to larger shear parameter along with more intense competition between participating modes.

VIV, as a nonlinearly coupling of structural and fluid dynamics, presents some interesting and complicated phenomena such as self-limited, self-excitation, jump of displacement between different branches and the hysteresis in lock-in region. It is still difficult for the prediction approach to capture all these VIV's traits, particularly the nonlinear jump or irregularities of VIV[14,15,23]. Therefore, further studies on better prediction model and deeper insight of multi-mode VIV remain to be done.

Acknowledgements

This work is supported by the National Natural Sciences Foundation (Grant No. 11232012 and 11372320).

References

[1] Mukhopadhyay A, Venugopal P, Vanka SP (1999) Numerical Study of Vortex Shedding From a Circular Cylinder in Linear Shear Flow. Journal of Fluid Engineering, Transactions of the ASME 121: 460-468.

[2] Lucor D, Imas L, Karniadakis GE (2001) Vortex dislocations and force distribution of a long flexible cylinders subjected to sheared flows. Journal of Fluids and Structures Mechanics 15: 641-650.

[3] Chen WM, Li M, Zhang LW, Tan TC, (2016) Study on Multi-mode VIV of Deepwater Riser in Different Flow Fields by Finite Element Simulations. J. of Offshore Mechanics and Arctic Engineering 138(1):1-8.

[4] Huse E, Kleiven G, Nielsen FG (1998) Large scale model testing of deep sea risers. In: Proceedings of the Offshore Technology Conference, Houston, Texas, OTC 8701.

[5] Lie H, Kaasen H K (2006) Model analysis of measurements from a large-scale VIV model test of a riser in linearly sheared flow, Journal of Fluid and Structures 22: 557-575.

[6]Tang YG, Zhang SX, Zhang RY, Liu HX (2007) Development of study on the dynamic characteristics of deep water mooring system, Journal of Marine Science and Application 6(3): 17-23

[7]Srinil N (2010) Multi-mode interactions in vortex-induced vibrations of flexible curved/straight structures with geometric nonlinearities. Journal of Fluids and Structures 26:1098-1122.

[8]Huera-Huarte FJ, Bearman PW, Chaplin JR (2006) On the force distribution along the axis of a flexible circular cylinder undergoing multi-mode vortex-induced vibrations, Journal of Fluids and Structures 22: 897~903.

[9]Huang S, Khorasanchi M, Herfjord K, (2011) Drag amplification of long flexible riser models undergoing multi-mode VIV in uniform currents. Journal of Fluids and Structures 27: 342-353.

[10]Jaiswal V, Vandiver JK, (2007) VIV response prediction for long risers with variable damping. Proceedings of the 26th International Conference on Offshore Mechanics and Arctic Engineering OMAE2007-29353:1-9.

[11]Tognarelli MA, Slocum ST, Frank WR, Campbell RB (2004) VIV response of a long flexible cylinder in uniform and linearly sheared currents. Offshore Technology Conference. OTC-16338, 1-12.

[12]Marcollo H, Hinwood JB (2002) A facility for evaluation of modal competition in an elastic riser. Proceedings of the twelfth (2002) international offshore and polar engineering conference Kitakyushu, Japan, May 26-31

[13]Zhang J, Tang YG, Huang L, Li W (2013) Multi-mode coupled vibration behavior of a deep-water riser under parametric excitations. Journal of Vibration and Shock 32(19): 51-56. In Chinese.

[14]Vandiver JK, Allen D, Li L (1996) The occurrence of lock-in under highly sheared conditions. Journal of Fluids and Structures 10:555-561.

[15]Sarpkaya T (2004) A Critical review of the intrinsic nature of vortex-induced vibration. Journal of Fluids and Structures Mechanics 19: 389-447.

[16]Vandiver JK, Li L (1999) SHEAR7 program theory manual. In MIT, Department of Ocean Engineering.

[17]Violette R, de Langre E, Szydlowski J (2010) A linear stability approach to vortex-induced vibrations and waves. Journal of Fluids and Structures 26 (3): 442-466.

[18]Facchinetti M (2004) Vortex-induced traveling waves along a cable. European J. of Mech. B/Fluids 16: 199~208.

[19]Huera-Huarte J, Bearman PW (2009) Wake structures and vortex-induced vibrations of a long flexible cylinder- Part 2: drag coefficients and vortex modes. Journal of Fluids and Structures 25(6): 991-1006.

[20]Chen WM, Li M, Zheng ZQ (2012) Dynamic Characteristics and VIV of Deepwater Riser with Axially Varying Structural Properties. Ocean Engineering 42:7-12.

[21]Chaplin JR, Bearman PW, Huera-Huarte FJ, Pattenden RJ (2005) Laboratory measurements of vortex-induced vibrations of a vertical tension riser in a stepped current. Journal of Fluids and Structures 21:3-24.

[22]Trim AD, Braaten H, Lie H et al. (2005) Experimental investigation of vortex-induced vibration of long marine risers. Journal of Fluids and Structures 21: 335-361.

[23]Bourguet R, Karniadakis GE, Triantafyllou MS (2013) Multi-frequency vortex-induced vibrations of a long tensioned beam in linear and exponential shear flows. Journal of Fluids and Structures 41:33-42.